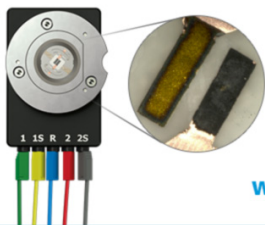


## Perspective—Mass Conservation in Models for Electrodeposition/Stripping in Lithium Metal Batteries

To cite this article: Lubhani Mishra *et al* 2021 *J. Electrochem. Soc.* **168** 092502

View the [article online](#) for updates and enhancements.

**Visualize the processes inside your battery!**  
**Discover the new ECC-Opto-10 and PAT-Cell-Opto-10 test cells!**



- Battery test cells for optical characterization
- High cycling stability, advanced cell design for easy handling
- For light microscopy and Raman spectroscopy

[www.el-cell.com](http://www.el-cell.com) +49 (0) 40 79012 734 [sales@el-cell.com](mailto:sales@el-cell.com)

**EL-CELL**<sup>®</sup>  
electrochemical test equipment





## Perspective—Mass Conservation in Models for Electrodeposition/Stripping in Lithium Metal Batteries

Lubhani Mishra,<sup>1,3,\*</sup> Akshay Subramaniam,<sup>2,\*</sup> Taejin Jang,<sup>1,3,\*</sup> Krishna Shah,<sup>1,4,\*</sup> Maitri Uppaluri,<sup>1,3,\*</sup> Scott A. Roberts,<sup>5,\*</sup> and Venkat R. Subramanian<sup>1,3,\*\*,z</sup>

<sup>1</sup>Walker Department of Mechanical Engineering, Texas Materials Institute, The University of Texas at Austin, Austin, Texas 78712, United States of America

<sup>2</sup>Department of Chemical Engineering, University of Washington, Seattle, Washington 98195, United States of America

<sup>3</sup>Materials Science and Engineering Program, Texas Materials Institute, The University of Texas at Austin, Austin, Texas 78712, United States of America

<sup>4</sup>Department of Mechanical Engineering, University of Alabama, Tuscaloosa, Alabama 35401, United States of America

<sup>5</sup>Thermal/Fluid Component Sciences Department, Engineering Sciences Center, Sandia National Laboratories, Albuquerque, New Mexico 87123, United States of America

Electrochemical models at different scales and varying levels of complexity have been used in the literature to study the evolution of the anode surface in lithium metal batteries. This includes continuum, mesoscale (phase-field approaches), and multiscale models. In this paper, using a motivating example of a moving boundary model in one dimension, we show how battery models need proper formulation for mass conservation, especially when simulated over multiple charge and discharge cycles. The article concludes with some thoughts on mass conservation and proper formulation for multiscale models.

© 2021 The Electrochemical Society ("ECS"). Published on behalf of ECS by IOP Publishing Limited. [DOI: 10.1149/1945-7111/ac2091]

Manuscript submitted July 9, 2021; revised manuscript received August 17, 2021. Published September 6, 2021.

Undoubtedly, lithium metal batteries have recently emerged as one of the most promising electrochemical energy storage technologies. This has brought significant attention to the development of this battery technology into a commercially viable battery system. However, this will require overcoming some key issues like uneven lithium metal deposition, dendrite formation, the evolution of "dead" lithium, and volume expansion. These shortcomings lead to poor cycle life, low columbic efficiency, and safety related concerns. Thus, several works<sup>1–6</sup> have aimed to develop various mathematical models based on the moving boundary approach for predicting changes in lithium morphology. These modeling frameworks can play a crucial role in enhancing our fundamental understanding of the transport and reaction mechanisms and guiding experimentalists in developing safer and more efficient lithium metal anodes. Models have been developed for mesoscale simulations, understanding mechanical effects, and phase-field simulations have been reported as well.<sup>3,7–10</sup>

In this work, we aim to bring attention to mass conservation in electrochemical models involving moving boundaries, which if ignored, might lead to erroneous results for the variables of interest in a battery, and in turn affect the accuracy of predictions for battery degradation and cycle life. Further, we observe that models are typically simulated for one cycle of plating and stripping processes (charge followed by discharge) in a lithium metal anode battery, and the potential mass conservation issues may only lead to a noticeable error during cycling. Multi-cycle battery simulations further necessitate the careful implementation of the mass balance in the electrochemical model to prevent cumulative error owing to mass accumulation (or depletion) in the system.

### Current status

This work builds on several past studies<sup>1,11–13</sup> where one-dimensional transport models have been developed to capture the movement of lithium during cycling. Lately, these models were studied and cycled at various rates, and it was observed that their imperfect mass conservation is too significant to be ignored, especially for repeated charge/discharge cycles. In this paper, we present the comparative results obtained after a careful implementation of an improved mass conservation formulation at the moving boundary at the electrode-electrolyte

interface. The one-dimensional transport model example has been chosen as a simple case to demonstrate and emphasize the importance of electrode-electrolyte interface mass balance and can be extended to detailed multiscale and multiphysics battery models.

**Motivating example: One-dimensional transport model for lithium-metal batteries.**—The following example deals with the one-dimensional mass transport in the separator region filled with a binary electrolyte in a lithium metal battery. Only the separator domain is modeled where its interface with the lithium metal anode is initially at  $x = 0$  and a constant current density is considered at the other end of the separator domain ( $x = L$ ) as shown in Fig. 1. The electrolyte consists of  $\text{Li}^+$  ions which undergo reduction and lithium metal plates at the anode having an initial "seed" lithium deposit of  $1 \mu\text{m}$ .

The model chosen is based on the assumption that the solid lithium metal is expanding into the separator and the total separator thickness decreases with time during charging. The reverse is assumed to be true during the discharge. Thus, the chosen separator or the liquid domain is perfectly compressive according to our model. This provides our model the flexibility to handle  $x = L$  either as separator/cathode interface or separator/lithium-metal interface (symmetric electrodes). Adding more detailed mechanics of the interface is beyond the scope of this paper.

This anode charging process has been modeled using the following equations:

For a binary electrolyte, the material balance of the ionic species can be written using the Nernst-Planck equation in one-dimension as:<sup>14</sup>

$$\frac{\partial c_i}{\partial t} = -D_i \frac{\partial}{\partial x} \left( -\frac{\partial c_i}{\partial x} - z_i \frac{F}{RT} c_i \frac{\partial \phi}{\partial x} \right), \quad i = 1, 2 \quad [1]$$

The assumption for electroneutrality in above Eq. 1 can be simplified as  $c_1 = c_2 = c$  and we get the following coupled set of equations for the mass transport within the electrolyte:

$$\frac{\partial c}{\partial t} = -D_1 \frac{\partial}{\partial x} \left( -\frac{\partial c}{\partial x} - \frac{F}{RT} c \frac{\partial \phi}{\partial x} \right) \quad [2]$$

$$\frac{\partial c}{\partial t} = -D_2 \frac{\partial}{\partial x} \left( -\frac{\partial c}{\partial x} + \frac{F}{RT} c \frac{\partial \phi}{\partial x} \right) \quad [3]$$

For further mathematical simplification of these equations, we have assumed constant electrolyte diffusivities for both anion and cation, i.e., ( $D_1 = D_2 = D$ ) which leads to the following decoupled equations

\*Electrochemical Society Member.

\*\*Electrochemical Society Fellow.

<sup>z</sup>E-mail: venkat.subramanian@utexas.edu

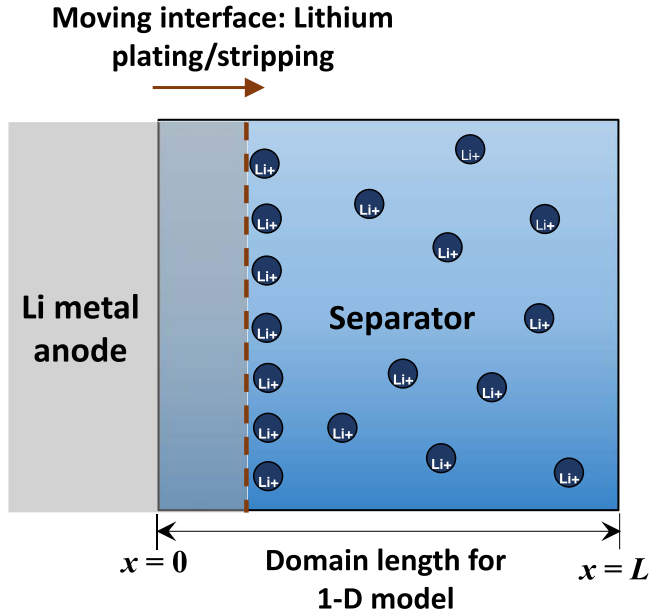


**Figure 1.** Schematic for the one-dimensional moving boundary model for electrodeposition/stripping in lithium metal batteries.

for the concentration and potential within the electrolyte. An alternate simplification using effective electrolyte diffusivity<sup>11,12,14</sup> can also be used to arrive at models that use effective diffusivity. We aim to keep the model as simple as possible to convey the relevant message of error in mass conservation. Mass leakage/accumulation was observed irrespective of this assumption. A simple version of the Maple code can be obtained from the corresponding author's website.<sup>15</sup> Different values of  $D_1$  and  $D_2$  can be provided in the code to study the effect of different diffusivities for cationic and anionic species.

$$\frac{\partial c}{\partial t} = D \frac{\partial^2 c}{\partial x^2} \quad [4]$$

$$0 = \frac{\partial}{\partial x} \left( c \frac{\partial \phi}{\partial x} \right) \quad [5]$$

At the electrode-electrolyte interfaces, the anionic flux is zero, i.e.,  $N_2 = 0$ . Thus, the boundary conditions can be interpreted in the following form:

At  $x = 0$  and  $L$ ,

$$\left. \begin{array}{l} N_1 = \frac{i}{F} \\ N_2 = 0 \end{array} \right\} \Rightarrow \left. \begin{array}{l} -D \frac{\partial c}{\partial x} - \frac{DF}{RT} c \frac{\partial \phi}{\partial x} = \frac{i}{F} \\ -D \frac{\partial c}{\partial x} + \frac{DF}{RT} c \frac{\partial \phi}{\partial x} = 0 \end{array} \right\} \Rightarrow \frac{\partial c}{\partial x} = -\frac{i}{2FD}, \quad c \frac{\partial \phi}{\partial x} = -\frac{i}{2FD} \left( \frac{RT}{F} \right) \quad [6]$$

Equation 6 is commonly reported in the literature and is perhaps built on the past literature for deposition<sup>13</sup> for models that mainly involve primary and secondary current distributions in electrochemical systems,<sup>1</sup> i.e., situations in which concentration gradients are ignored.

Now, the kinetics at the anode-electrolyte interface for small magnitudes of overpotential is governed by the modified Butler-Volmer kinetics as:

$$i_{BV} = i_0 \left( \frac{c}{c_0} \right)^{0.5} \frac{\eta F}{RT} \quad [7]$$

where the equilibrium potential,  $E_{eq}$  is considered to be zero in the expression for activation overpotential,  $\eta$  and the reference electrode potential,  $V_a$  is set as zero. This form of the kinetics term was chosen

to facilitate numerical simulation and avoiding Butler-Volmer kinetics in the Newton-Raphson iteration (the chosen model is still nonlinear because of concentration-potential coupling).

$$\eta = V_a - \phi - E_{eq} \quad [8]$$

A uniform current density,  $i_{app}$  is assumed at the other end of the separator at  $x = L$ .

The velocity of the moving boundary at the anode is prescribed as:<sup>13</sup>

$$u_x = \frac{ds}{dt} = -\frac{M_w i_{BV}}{\rho F} \quad [9]$$

The initial conditions for the system of equations are given as  $c(x,0) = c_0$ . We also take the initial position of the interface to be  $s(0) = 1 \mu\text{m}$ , corresponding to an initial deposit "seed."

Equations 4–9 along with the appropriate boundary conditions can be solved numerically by using standard numerical approaches. In order to emphasize on the appropriate mass conservation formulation, let us consider the boundary conditions in Eq. 6 in **Model 1** and the modified boundary conditions in **Model 2**.

**Model 1.**—From Eq. 6, the boundary conditions take the following final form:

$$\begin{aligned} \text{At } x = 0, \quad \frac{\partial c}{\partial x} &= -\frac{i_{BV}}{2FD} \\ c \frac{\partial \phi}{\partial x} &= -\frac{i_{BV}}{2FD} \left( \frac{RT}{F} \right) \end{aligned} \quad [10]$$

$$\begin{aligned} \text{At } x = L, \quad \frac{\partial c}{\partial x} &= -\frac{i_{app,LCrate}}{2FD} \\ c \frac{\partial \phi}{\partial x} &= -\frac{i_{app,LCrate}}{2FD} \left( \frac{RT}{F} \right) \end{aligned} \quad [11]$$

The simulation results for these model equations over several cycles indicated the accumulation of mass in the system domain along with some indication for the battery degradation as shown in Fig. 2. The results for electrolyte concentration and potential for Model 1 are plotted for over 50 cycles at the moving boundary (and also shown separately for 1st cycle: charging followed by discharging). It can be clearly observed that the electrolyte concentration at anode increases continuously with the increase in cycles. This is also responsible for the decay in the electrolyte potential with the increase in cycles as seen in Fig. 2b. The results obtained from Model 1 highlight the importance of conserving mass in model development. Thus, we suggest the modification of the flux boundary conditions in Model 2 as described below.

**Model 2.**—It should be noted that the boundary conditions at the moving boundary at  $x = 0$  account for the interface transport. To conserve the mass at the moving interface, an additional advective flux term is added which compensates for the diffusant disappearing from the electrolyte domain. This formulation is based on the mass jump condition at the moving interfaces.<sup>16</sup>

Using Eq. 6, we have now included advective flux at  $x = 0$ ,

$$\begin{aligned} \left. \begin{array}{l} N_1 = \frac{i}{F} + cv_n \\ N_2 = cv_n \end{array} \right\} \Rightarrow \left. \begin{array}{l} -D \frac{\partial c}{\partial x} - \frac{DF}{RT} c \frac{\partial \phi}{\partial x} = \frac{i}{F} + cv_n \\ -D \frac{\partial c}{\partial x} + \frac{DF}{RT} c \frac{\partial \phi}{\partial x} = cv_n \end{array} \right\} \\ \Rightarrow \frac{\partial c}{\partial x} = -\frac{i}{2FD} - \frac{cv_n}{D}, \quad c \frac{\partial \phi}{\partial x} = -\frac{i}{2FD} \left( \frac{RT}{F} \right) \end{aligned} \quad [12]$$

Thus, the modified boundary conditions in Model 2 can be implemented as follows:

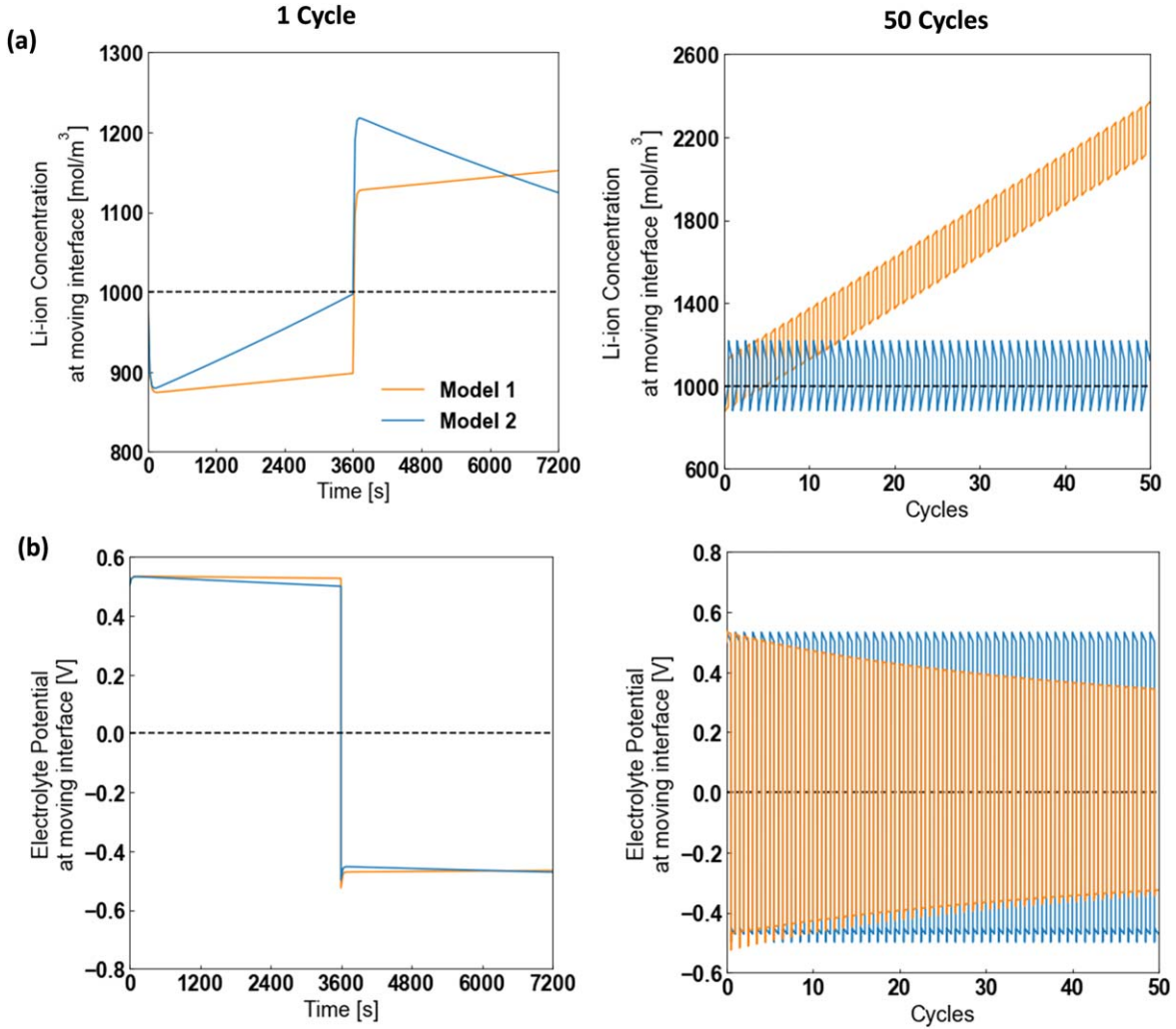


**Figure 2.** Comparative results for electrolyte (a) concentration and (b) potential over 50 cycles for the original model without advective flux (Model 1) and modified model with advective flux (Model 2) at moving interface at  $x = 0$ .

$$\begin{aligned} \text{At } x = 0, \quad \frac{\partial c}{\partial x} &= -\frac{i_{BV}}{2FD} - \frac{c v_n}{D} \\ c \frac{\partial \phi}{\partial x} &= -\frac{i_{BV}}{2FD} \left( \frac{RT}{F} \right). \end{aligned} \quad [13]$$

$$\begin{aligned} \text{At } x = L, \quad \frac{\partial c}{\partial x} &= -\frac{i_{app,1C} C_{rate}}{2FD} \\ c \frac{\partial \phi}{\partial x} &= -\frac{i_{app,1C} C_{rate}}{2FD} \left( \frac{RT}{F} \right) \end{aligned} \quad [14]$$

The results for the model equations, Eqs. 4–9 along with the modified boundary conditions, Eqs. 13–14 have been solved numerically and are shown in comparison with results for Model 1 in Fig. 2. Both electrolyte concentration and potential remain conserved over charge/discharge cycles while exhibiting the characteristic inverse signatures as seen in the results for one cycle. In other words, Fig. 2 shows the comparative results for the two cases of Models 1 and 2 where the difference lies in accounting for the appropriate concentration flux in the boundary conditions at the moving boundary.

Additional results are shown in Figs. 3a–3b for the average and total concentration in the entire separator domain to provide additional insights into the overall mass conservation. The variation in the location of the moving boundary is also included in Fig. 2c to compare Models 1 and 2.

The average concentration in the electrolyte is plotted in Fig. 3a. We can see that the modification of concentration boundary condition is needed for conserving the mass and average concentration goes back to the original concentration. Without this modification in the boundary condition, the average concentration increases after every cycle, creating issues over multiple cycles of charge and discharge. Figure 3b shows the total mass of lithium ions in the electrolyte (including the deposited/stripped solid phase). The appropriate mass balance at the moving interface is needed for proper conservation of mass. If ignored, for a single cycle, it is perhaps not a significant issue, but for repeated cycling, the error accumulates.

It is worthwhile to note that in both Models 1 and 2, the moving boundary is accurately predicted, and at the end of discharge, the moving anode/electrolyte boundary goes back to its original position (for the same rates and parameters for charge and discharge) as shown in Fig. 3c. This might give false confirmation for modelers who are only tracking the moving boundary growth in one- and two-dimensional models.

**Non-dimensionalization and numerical methodology.**—The governing equations, Eqs. 4–5, are rendered dimensionless using the scaled variables defined in Table I along with the boundary and initial conditions as listed below:

$$\frac{\partial C}{\partial \tau} = \frac{1}{\tau_D} \frac{\partial^2 C}{\partial X^2} \quad [15]$$

**Table I. Scaling variables used for non-dimensionalization.**

Scaling variables	
$X$	$=x/L$
$C$	$=c/c_0$
$\Phi$	$=\phi/\phi_0$
$V_a'$	$=V_a/\phi_0$
$\tau$	$=t/(3600/ Crate )$
$S$	$=s/L$
Dimensionless groups	
$\delta$	$=\frac{(i_{app,1C}LCrate)}{(2FDc_0)}$
$Da$	$=\frac{(i_0L)}{(2c_0DF)}$
$Pe$	$=\frac{(M_w/\rho)\cdot(i_03600)}{(LF Crate )}$
$\tau_D$	$=\frac{( Crate L^2)}{(3600D)}$
$\phi_0$	$=\frac{(RT)}{F}$

$$0 = \frac{\partial}{\partial X} \left( C \frac{\partial \Phi}{\partial X} \right) \quad [16]$$

**Model 1:** At  $X = 0$ ,  $\frac{\partial C}{\partial X} = -Da C^{0.5}(V_a' - \Phi)$

$$C \frac{\partial \Phi}{\partial X} = -Da C^{0.5}(V_a' - \Phi)$$

**Model 2:** At  $X = 0$ ,  $\frac{\partial C}{\partial X} = -Da C^{0.5}(V_a' - \Phi) + C(Pe \cdot C^{0.5}(V_a' - \Phi))$

$$C \frac{\partial \Phi}{\partial X} = -Da C^{0.5}(V_a' - \Phi) \quad [17]$$

$$\text{At } X = 1, \frac{\partial C}{\partial X} = -\delta$$

$$\Phi = 0 \quad [18]$$

$$\text{At } \tau = 0, C(X, 0) = 1 \quad [19]$$

$$\frac{\partial S}{\partial \tau} = -\frac{Pe}{\tau_D} C^{0.5}(V_a' - \Phi) \quad [20]$$

An inspection of the dimensionless equations, Eqs. 15–20, suggests that the mass and electric fields are governed by mainly two pertinent dimensionless groups, namely, Damköhler number ( $Da$ )

**Table II. Baseline parameters used in this study.**

Symbols	Parameters	Values	Units
Geometrical Parameters			
$L_x$	Domain length in x	50 e-6	m
Operational parameters			
$i_{app,1C}$	Applied current density	10	A m <sup>-2</sup>
$i_0$	Exchange current density	20	A m <sup>-2</sup>
$c_0$	Initial Concentration	1000	mol m <sup>-3</sup>
$T$	Operating temperature	298	K
Material parameters			
$D$	Diffusion coefficient	1e-11	m <sup>2</sup> s <sup>-1</sup>
$M$	Molar mass of Lithium	6.941	g mol <sup>-1</sup>
$\rho$	Density of Lithium	0.534	g cm <sup>-3</sup>
General parameters			
$R$	universal Gas Constant	8.314	J mol <sup>-1</sup> ·K <sup>-1</sup>
$F$	Faraday's Constant	96487	C mol <sup>-1</sup>

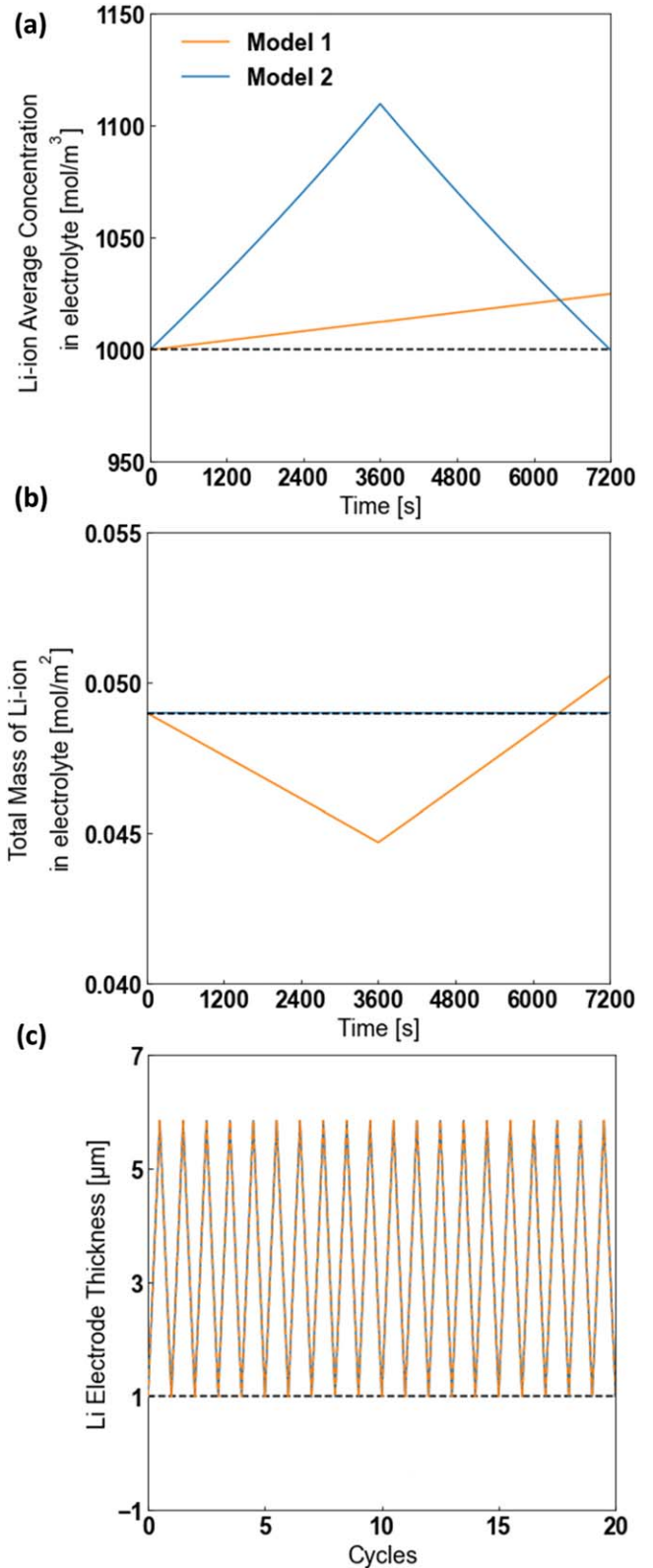


**Figure 3.** Comparative results for (a) average electrolyte concentration, (b) total mass of Li<sup>+</sup> ions in electrolyte, and (c) location of moving boundary for the original model without advective flux (Model 1) and modified model with advective flux (Model 2) in boundary conditions. (Dashed line indicates the baseline values)

and Peclet number ( $Pe$ ) defined in Table II. The effect of these dimensionless groups on mass conservation can be further delineated in a detailed fashion.

Table II enlists the baseline model parameters used for the reported simulation results in Figs. 2 and 3.

This model was further transformed to a fixed domain using Landau transformation<sup>17</sup> where  $Z$  is the transformed coordinate which fixes the position of the moving boundary at  $Z = 0$ :

$$Z = \frac{X - S(\tau)}{1 - S(\tau)} \quad [21]$$

The governing equations after Landau transformation are given as:

$$\frac{\partial C}{\partial \tau} = \frac{dS}{d\tau} \frac{(1-Z)}{(1-S)} \frac{\partial C}{\partial Z} + \frac{1}{\tau_D (S-1)^2} \frac{\partial^2 C}{\partial Z^2} \quad [22]$$

$$0 = \frac{\partial}{\partial Z} \left( C \frac{\partial \Phi}{\partial Z} \right) \quad [23]$$

The transformed boundary and initial conditions are:

$$\text{Model 1: At } Z = 0, \frac{\partial C}{\partial Z} = -Da C^{0.5} (V'_a - \Phi)$$

$$C \frac{\partial \Phi}{\partial Z} = -Da C^{0.5} (V'_a - \Phi)$$

$$\text{Model 2: At } Z = 0, \frac{\partial C}{\partial Z} = -Da C^{0.5} (V'_a - \Phi) + C(Pe \cdot C^{0.5} (V'_a - \Phi))$$

$$C \frac{\partial \Phi}{\partial Z} = -Da C^{0.5} (V'_a - \Phi) \quad [24]$$

$$\text{At } Z = 1, \frac{\partial C}{\partial Z} = -\delta(1-S) \\ \Phi = 0 \quad [25]$$

$$\text{At } \tau = 0, C(Z, 0) = 1 \quad [26]$$

Finally, the moving boundary velocity is given as below in transformed coordinates:

$$\frac{\partial S}{\partial \tau} = -\frac{Pe}{\tau_D} C^{0.5} (V'_a - \Phi) \quad [27]$$

The numerical results have been obtained using the method of lines approach. This is performed by discretizing the transformed equations, Eqs. 22–27 using a finite-difference discretization scheme and simulated in Maple's stiff DAE solver (Rosenbrock methods) aided by consistent initialization for the algebraic variables. The results were obtained for relative and absolute tolerances of 1e-6 and 1e-8, respectively. The results were also verified using finite element based solver, COMSOL Multiphysics.

### Future Needs and Prospects

- In this paper, a one-dimensional model was used to show the importance of proper formulation of the boundary conditions for mass conservation in lithium metal batteries.

- Some multidimensional and multiscale models have been reported in the literature. However, proper check of mass and charge conservation needs to be properly implemented. Otherwise, the addition of more complicated models may not produce meaningful results. We highly recommend checking and reporting mass and charge conservation of individual models and coupled multiscale for the first cycle before additional cycles are simulated.

- When multiscale models are developed, proper care should be taken to ensure mass and charge are conserved in each scale. For example, the modified moving boundary model presented here (Model 2) can be coupled with models in meso or other scales.

- Since the model considered in this paper is one-dimensional, Landau transformation was used for the numerical simulation. This transformation is not useful for two-dimensional models. Thus, the boundary conditions and model formulation should be based on physics. The choice of the numerical method to solve the model depends on the dimension and structure of the model and the physics.

In this manuscript, we took the approach of adding advection directly to the boundary conditions at the moving interface. We believe that the proposed model is perhaps the best possible model for moving boundaries. Moving the convection term to the bulk will make the model more restrictive for the choice of boundary conditions at  $x = L$ .







### Summary

We have presented a simple analysis for a one-dimensional moving boundary model to bring attention and provide emphasis on mass conservation in the models for lithium metal batteries. Traditional moving boundary battery models neglect the role of advection at the moving boundaries, introducing consistent and accumulating mass conservation errors that are, while potentially not significant for a single cycle, lead to significant accumulation of errors over multiple charge-discharge cycles. This proposition can be extended to multiscale and multiphysics models for advanced modeling of plating and stripping at lithium metal anodes using moving boundary models. Consistent implementations are crucial in all-encompassing numerical modeling frameworks around plating/stripping at lithium metal anodes.

### Acknowledgments

The authors would like to express gratitude to Assistant Secretary for Energy Efficiency and Renewable Energy, Office of Vehicle Technologies of the DOE through the Advanced Battery Material Research (BMR) Program (Battery500 consortium). This paper describes objective technical results and analysis. Any subjective views or opinions that might be expressed in the paper do not necessarily represent the views of the U.S. Department of Energy or the United States Government. Supported by the Laboratory Directed Research and Development program at Sandia National Laboratories, a multimission laboratory managed and operated by National Technology and Engineering Solutions of Sandia, LLC., a wholly owned subsidiary of Honeywell International, Inc., for the U.S. Department of Energy's National Nuclear Security Administration under contract DE-NA-0003525. The corresponding author, VS wants to acknowledge Dr. Harry Ploehn for teaching the concept of jump mass and momentum balances in his graduate transport course at the University of South Carolina.

### ORCID

Lubhani Mishra  <https://orcid.org/0000-0003-2135-9381>  
 Akshay Subramaniam  <https://orcid.org/0000-0002-9306-7436>  
 Taejin Jang  <https://orcid.org/0000-0003-4279-8455>  
 Krishna Shah  <https://orcid.org/0000-0002-7802-6361>  
 Maitri Uppaluri  <https://orcid.org/0000-0002-6612-3009>  
 Scott A. Roberts  <https://orcid.org/0000-0002-4196-6771>  
 Venkat R. Subramaniam  <https://orcid.org/0000-0002-2092-9744>

### References

1. C. Monroe and J. Newman, *J. Electrochem. Soc.*, **150**, A1377 (2003).
2. F. Hao, A. Verma, and P. P. Mukherjee, *ACS Appl. Mater. Inter.*, **10**, 26320 (2018).

3. Z. Hong and V. Viswanathan, *ACS Energy Lett.*, **3**, 1737 (2018).
4. G. Li and C. W. Monroe, *Annu. Rev. Chem. Biomol. Eng.*, **11**, 277 (2020).
5. A. Ferrese and J. Newman, *J. Electrochem. Soc.*, **161**, A948 (2014).
6. K. Shah, A. Subramaniam, L. Mishra, T. Jang, M. Z. Bazant, R. D. Braatz, and V. R. Subramanian, *J. Electrochem. Soc.*, **167**, 133501 (2020).
7. X. Zhang, Q. J. Wang, K. L. Harrison, K. Jungjohann, B. L. Boyce, S. A. Roberts, P. M. Attia, and S. J. Harris, *J. Electrochem. Soc.*, **166**, A3639 (2019).
8. X. Zhang, Q. J. Wang, K. L. Harrison, S. A. Roberts, and S. J. Harris, *Cell Rep. Phys. Sci.*, **1**, 100012 (2020).
9. P. Barai, K. Higa, and V. Srinivasan, *J. Electrochem. Soc.*, **165**, A2654 (2018).
10. L. Gao and Z. Guo, *Comput. Mater. Sci.*, **183**, 109919 (2020).
11. M. Uppaluri, A. Subramaniam, L. Mishra, V. Viswanathan, and V. R. Subramanian, *J. Electrochem. Soc.*, **167**, 160547 (2020).
12. A. Subramaniam, J. Chen, T. Jang, N. R. Geise, R. M. Kasse, M. F. Toney, and V. R. Subramanian, *J. Electrochem. Soc.*, **166**, A3806 (2019).
13. R. Alkire, T. Bergh, and R. L. Sani, *J. Electrochem. Soc.*, **125**, 1981 (1978).
14. J. Newman and K. E. Thomas-Alyea, *Electrochemical Systems* (Wiley, Hoboken, NJ) 3rd ed. (2004).
15. <http://sites.utexas.edu/maple/models-codes-2/>.
16. W. M. Deen, *Analysis of Transport Phenomena* (Oxford University Press, New York, NY) 2nd ed. (2012).
17. H. G. Landau, *Q. Appl. Math.*, **8**, 81 (1950).